1 Supplementary Methods

1.1 Derivation test of the BBLS calculation

In the Methods, we proposed an extension of the standard branch length score (BLS) by incorporating the uncertainty associated with determining motif instances at the leaf nodes,

$$BBLS(p_V) = \sum_{\sigma_V} P(\sigma_V) BLS(\sigma_V) \tag{1}$$

where $V = \{1, 2, \cdots, n\}$ is the set of leaf nodes in the tree. $p_V = (p_1, p_2, \cdots, p_n)$ with $p_i \equiv P(\sigma_i = 1)$, denoting the probability of the sequence in node i containing a motif site. $P(\sigma_V) \equiv \prod_{i=1}^{n}[\sigma_i p_i + (1-\sigma_i)(1-p_i)]$, and $BLS(\sigma_V)$ is the branch length score of the set of leaf nodes with $\sigma_i = 1$ for all $i \in V$. Note that $BLS(\sigma_V)$ is zero if $\sum_{i \in V} \sigma_i \leq 1$.

Let $MRCA(\sigma_V)$ denote the most recent common ancestor (MRCA) of the leaf nodes in V with $\sigma_i = 1$. $BLS(\sigma_V)$ is then the total branch length of the subtree that connects $MRCA(\sigma_V)$ and all leaf nodes with $\sigma_i = 1$ for all $i \in V$.

Eq. (1) involves the summation of 2^n terms, corresponding to all possible 0-1 configurations of the leaf nodes. In general, it can not be directly applied for computing $BBLS(p_V)$ when n is large. However, we note that there are at most $n-1$ MRCAs involved in the summation, and we can regroup terms in Eq. (1) according to which MRCA is used, which leads to

$$BBLS(p_V) = \sum_{i=n+1}^{N} P(MRCA = i) L(T_i | MRCA = i). \tag{2}$$

where $N = 2n-1$ is the total number of nodes in the tree, $P(MRCA = i)$ is the probability of the MRCA being node i, and $L(T_i | MRCA = i)$ is the BBLS of the subtree T_i conditioned on $MRCA = i$.

$P(MRCA = i)$ can be calculated according to

$$P(MRCA = i) = P(\sigma_{c^1(i)} = 1) P(\sigma_{c^2(i)} = 1) P(\sigma_{T_i^c} = 0) \tag{3}$$

that is, the product of the probabilities that both of its two child nodes are in state 1 and all leaf nodes that are not descendent of i are in state 0. Both $P(\sigma_i = 1)$ and $P(\sigma_{T_i^c} = 0)$ can be calculated efficiently using the following recursion:

$$\begin{aligned} P(\sigma_i = 1) &= 1 - [1 - P(\sigma_{c^1(i)} = 1)][1 - P(\sigma_{c^2(i)} = 1)] \qquad (4) \\ P(\sigma_{T_i^c} = 0) &= P(\sigma_{T^c_{\pi(i)}} = 0)[1 - P(\sigma_{s(i)} = 1)] \qquad (5) \end{aligned}$$

where $s(i)$ denotes the sister node of node i. For a given binary assignment σ_V of the leaf nodes, Eq. (4) propogates σ toward the root using the OR operator.

$L(T_i|MRCA = i)$ is the BBLS of the subtree T_i conditioned on $MRCA = i$. Since node i is a MRCA, both of its two child nodes are included in the subtree T_i, that is, $L(T_i|MRCA = i)$ includes the summation of $l_{c^1(i)}$ and $l_{c^2(i)}$ (l_i is the length of the edge leading to node i). In addition, the edges contained in the two subtrees of $c^1(i)$ and $c^2(i)$ have also to be included:

$$L(T_i|MCRA = i) = l_{c^1(i)} + l_{c^2(i)} + L(T_{c^1(i)}|\sigma_{c^1(i)} = 1) + L(T_{c^2(i)}|\sigma_{c^2(i)} = 1) \qquad (6)$$

where we have used $L(T_k|\sigma_k = 1)$ to denote the BBLS of the subtree T_k conditioned on node k being in state 1 ($\sigma_k = 1$). The condition $\sigma_k = 1$ specifies that at least one of the child nodes of k has to be in state 1, which can be either node $c^1(k)$ or $c^2(k)$, or both. Therefore, $L(T_k|\sigma_k = 1)$ can be calculated recursively according to

$$\begin{aligned} L(T_k|\sigma_k = 1) &= [P(\sigma_{c^1(k)} = 1)P(\sigma_{c^2(k)} = 0)(l_{c^1(k)} + L(T_{c^1(k)}|\sigma_{c^1(k)} = 1)) + \\ &\quad P(\sigma_{c^1(k)} = 0)P(\sigma_{c^2(k)} = 1)(l_{c^2(k)} + L(T_{c^2(k)}|\sigma_{c^2(k)} = 1)) + \\ &\quad P(\sigma_{c^1(k)} = 1)P(\sigma_{c^2(k)} = 1)(l_{c^1(k)} + L(T_{c^1(k)}|\sigma_{c^1(k)} = 1) + \\ &\quad l_{c^2(k)} + L(T_{c^2(k)}|\sigma_{c^2(k)} = 1))]/P(\sigma_k = 1) \qquad (7) \\ &= [P(\sigma_{c^1(k)} = 1)(l_{c^1(k)} + L(T_{c^1(k)}|\sigma_{c^1(k)} = 1)) + \\ &\quad P(\sigma_{c^2(k)} = 1)(l_{c^2(k)} + L(T_{c^2(k)}|\sigma_{c^2(k)} = 1))]/P(\sigma_k = 1) \qquad (8) \end{aligned}$$

If the effective branch length l_k^* is defined to be

$$l_k^* = l_k + L(T_k|\sigma_k = 1) \qquad (9)$$

then we have the following recurrence for calculating l_k^*

$$l_k^* = l_k + [P(\sigma_{c^l(k)} = 1)l^*_{c^1(k)} + P(\sigma_{c^2(k)} = 1)l^*_{c^2(k)}]/P(\sigma_k = 1) \qquad (10)$$

Consequently, the BBLS in Eq. (2) can be calculated using:

$$BBLS(p_V) = \sum_{i=n+1}^{N} P(\sigma_{c^1(i)} = 1)P(\sigma_{c^2(i)} = 1)P(\sigma_{T_i^c} = 0)(l^*_{c^1(i)} + l^*_{c^2(i)}) \tag{11}$$

Note that to calculate each of the equations in 4, 5, and 11, we only need to traverse the tree once. Therefore, the new algorithm for calculating BBLS scale only linearly with the number of nodes in the tree.

1.2 An example

Next we illustrate the calculation of BBLS derived in Eq. (11) using an example phylogenetic tree shown in Figure 1. The tree consists of $n = 4$ leaf nodes and 3 ancestral nodes. The probability of the leaf nodes being in state 1 is specified by $p_i = P(\sigma_i = 1)$ for leaf node i. For simplicity, we have chosen $p_i = 1/2$ for all $i = 1, \cdots, n$.

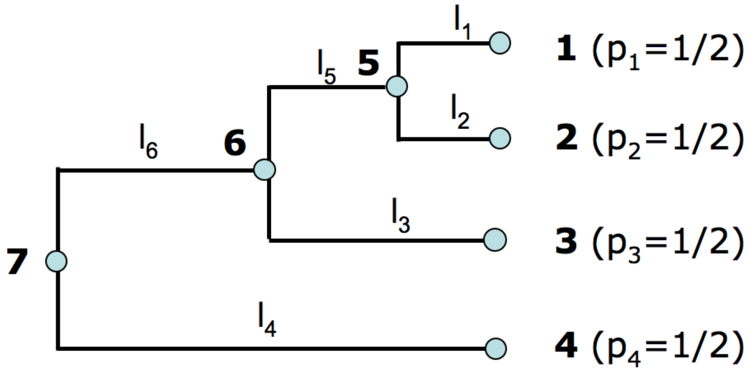

Figure 1: An example phylogenetic tree.

Next we first show detailed steps of calculating BBLS using Eq. (1), and then demonstrate how to calculate BBLS using Eq. (11) and compare the results obtained from the two approaches.

1.2.1 Computing BBLS according to Eq. (1)

Under this approach, we list all potential combinations of leaf nodes and calculate their probabilities and their corresponding branch length scores. The phylogenetic tree in Figure 1 consists of 16 possible 0-1 configurations of the leaf nodes, with 11 configurations consisting of at least two 1s. The complete list of these combinations and their corresponding branch length scores are shown in the following table:

σ_1	σ_2	σ_3	σ_4	Prob	BLS
1	1	0	0	1/16	$l_1 + l_2$
1	0	1	0	1/16	$l_1 + l_3 + l_5$
1	0	0	1	1/16	$l_1 + l_4 + l_5 + l_6$
0	1	1	0	1/16	$l_2 + l_3 + l_5$
0	1	0	1	1/16	$l_2 + l_4 + l_5 + l_6$
0	0	1	1	1/16	$l_3 + l_4 + l_6$
1	1	1	0	1/16	$l_1 + l_2 + l_3 + l_5$
1	1	0	1	1/16	$l_1 + l_2 + l_4 + l_5 + l_6$
1	0	1	1	1/16	$l_1 + l_3 + l_4 + l_5 + l_6$
0	1	1	1	1/16	$l_2 + l_3 + l_4 + l_5 + l_6$
1	1	1	1	1/16	$l_1 + l_2 + l_3 + l_4 + l_5 + l_6$

According to Eq. (1), BBLS is the sum of the BLS shown in the last column of the above table, weighted by their corresponding probabilities in the second last column. This leads to

$$BBLS = \frac{1}{16}[7(l_1 + l_2 + l_3 + l_4 + l_6) + 9l_5] \tag{12}$$

1.3 Computing BBLS according to Eq. (11)

To apply Eq. (11), we first calculate $P(\sigma_i = 1)$ and $P(\sigma_{T_i^c} = 0)$ for $i = 5$ and 6:

$$p_5 = P(\sigma_5 = 1) = 1 - (1 - p_1)(1 - p_2) = 3/4 \tag{13}$$

$$p_6 = P(\sigma_6 = 1) = 1 - (1 - p_3)(1 - p_5) = 7/8 \tag{14}$$

$$P(\sigma_{T_6^c} = 0) = P(\sigma_4 = 0) = 1/2 \tag{15}$$

$$P(\sigma_{T_5^c} = 0) = P(\sigma_{T_6^c} = 0)P(\sigma_3 = 0) = 1/4 \tag{16}$$

Next we calculate the effective branch length:

$$l_5^* = l_5 + (p_1 l_1 + p_2 l_2)/p_5 = l_5 + \frac{2}{3}(l_1 + l_2) \quad (17)$$

$$l_6^* = l_6 + (p_5 l_5^* + p_3 l_3)/p_6 = l_6 + \frac{2}{7}(2l_1 + 2l_2 + 2l_3 + 3l_5) \quad (18)$$

There are thee potential MRCAs (5, 6 and 7) in the phylogenetic tree in Figure 1. Applying Eq. (11), we then have

$$\begin{aligned} BBLS &= \sum_{i=5}^{7} p_{c^1(i)} p_{c^2(i)} P(\sigma_{T_i^c} = 0)(l^*_{c^1(i)} + l^*_{c^2(i)}) && (19) \\ &= \frac{1}{16}(l_1 + l_2) + \frac{3}{16}(l_3 + l_5^*) + \frac{7}{16}(l_4 + l_6^*) && (20) \\ &= \frac{1}{16}[7(l_1 + l_2 + l_3 + l_6) + 9l_5] && (21) \end{aligned}$$

which is the same as the BBLS derived from the first approach shown in Eq. (12).

1.4 Log likelihood ratio $\log(P(x_i|x_{\pi(i)}, \sigma_i = 1)/P(x_i|x_{\pi(i)}, \sigma_i = 0))$

Consider the branch connecting the parent node $\pi(i)$ to its child node i. If the sequences in the two nodes (denoted by $x_{\pi(i)}$ and x_i respectively) are conserved, we suggest in the Methods that the log likelihood ratio score $\log(P(x_i|x_{\pi(i)}, \sigma_i = 1)/P(x_i|x_{\pi(i)}, \sigma_i = 0))$ under the constrained model vs. neutral model should approximately scale linearly with the branch length (l_i) between node $\pi(i)$ and node i. Next we provide an explanation for this approximation.

Suppose the sequence evolution along the branch is modeled by the Jukes-Cantor model. For simplicity of discussion, we assume that the conserved sequences in the two nodes are identical ($x_i = x_{\pi(i)}$). According to the Jukes-Cantor model, the chance of a sequence remaining unchanged over a period of $T = l_i$ time units under the neutral evolution is

$$P(x_i|x_{\pi(i)}, \sigma_i = 0) = \frac{1}{4}(1 + 3e^{-4\alpha l_i}) \quad (22)$$

where α is a rate parameter of the neutral evolution. For the evolution of the constrained sequence, it is often modeled by a slower rate of evolution, that is, to multiply the parameter α

with a number $\gamma < 1$, which leads to

$$P(x_i|x_{\pi(i)}, \sigma_i = 1) = \frac{1}{4}(1 + 3e^{-4\gamma\alpha l_i}) \tag{23}$$

The log ratio between the two likelihood is then

$$\begin{aligned}\log\frac{P(x_i|x_{\pi(i)}, \sigma_i = 1)}{P(x_i|x_{\pi(i)}, \sigma_i = 0)} &= \log\frac{1 + 3e^{-4\gamma\alpha T}}{1 + 3e^{-4\alpha T}} &(24)\\ &= 3\alpha(1-\gamma)T + O((\alpha T)^2) &(25)\\ &\sim T &(26)\end{aligned}$$

where the approximation holds when the expected number of substitutions over the branch is small, which is true for closely related species such as the mammalian species we are considering.

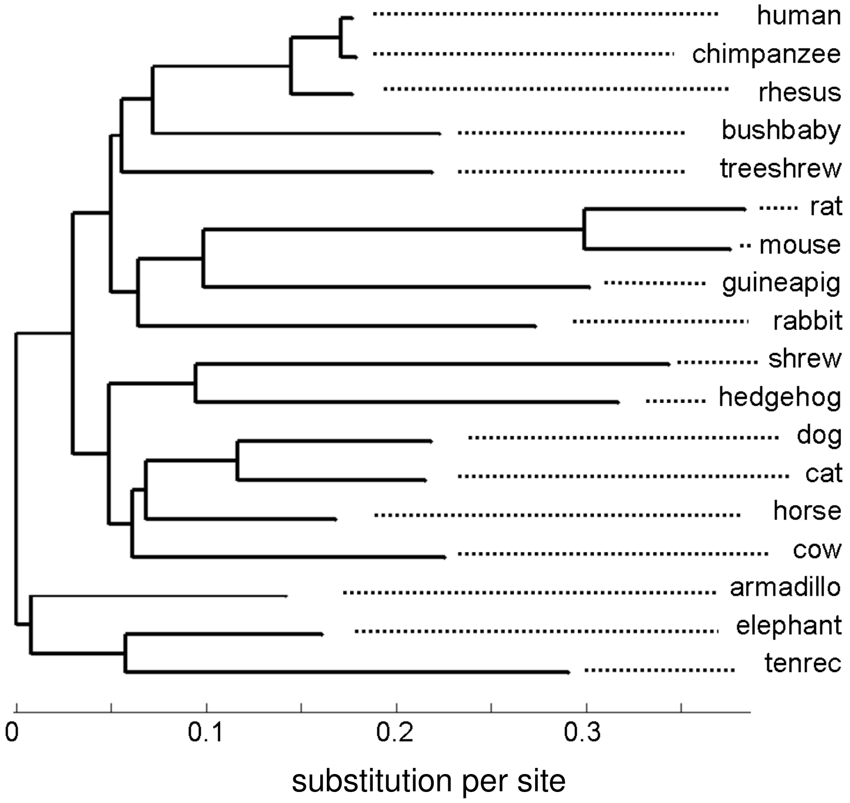

Figure S1 Phylogenetic tree of 18 placental mammals with genomes available.

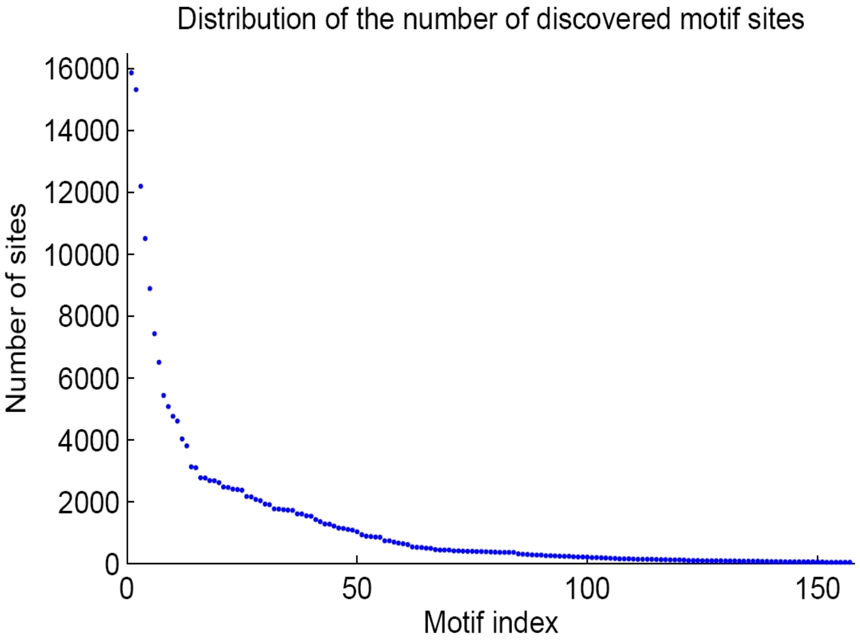

Figure S2 Number of discovered sites for the 157 motifs with FDR≤0.1. Each dot represents one motif.

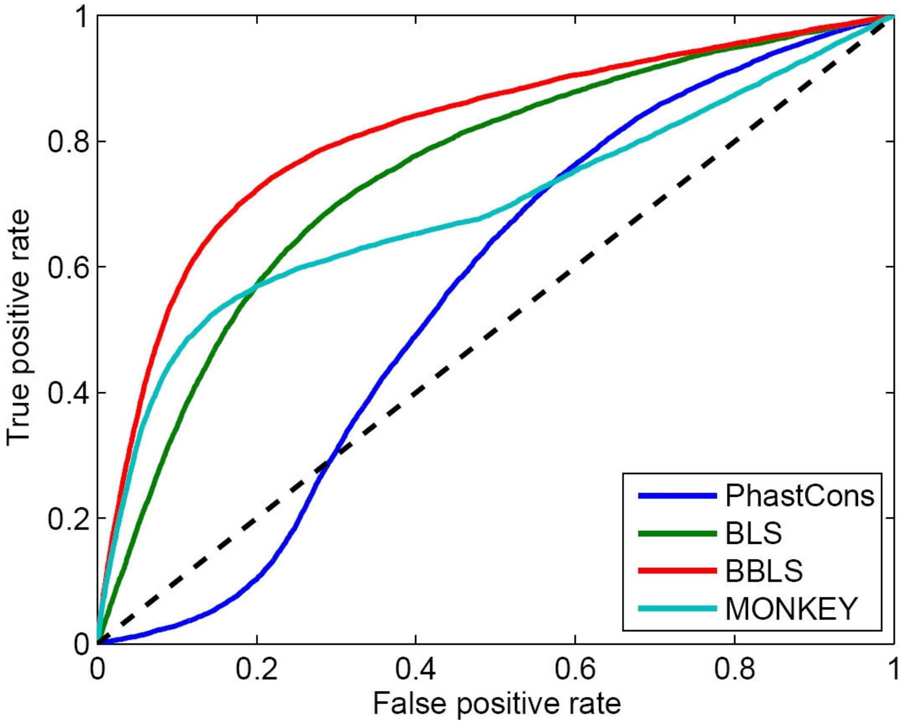

Figure S3 ROC curves of different methods for predicting **CTCF** binding sites. PhastCons: PhastCons conservation score; BLS: Branch length score; BBLS: Bayesian branch length score; MONKEY: Conservation p-value calculated by MONKEY (Moses et al., 2004). Experimentally identified CTCF sites are from Kim et al. (2007) and Barski et al. (2007).

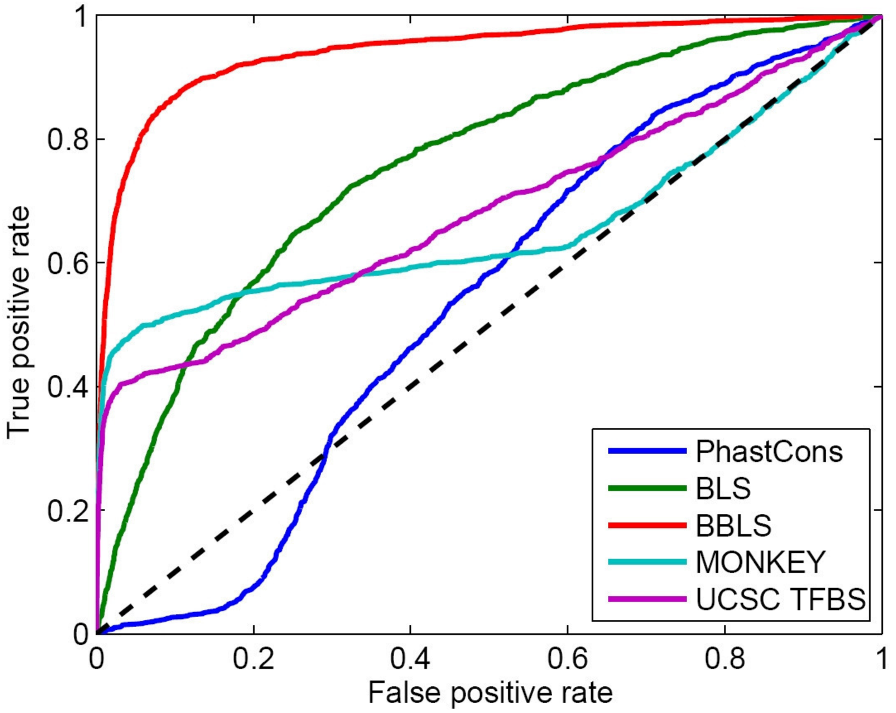

Figure S4 ROC curves of different methods for predicting **NRSE** binding sites. PhastCons: PhastCons conservation score; BLS: Branch length score; BBLS: Bayesian branch length score; MONKEY: Conservation p-value calculated by MONKEY (Moses et al., 2004); UCSC TFBS: Predicted sites from UCSC genome browser. Experimentally identified NRSE sites are from Johnson et al. (2006).

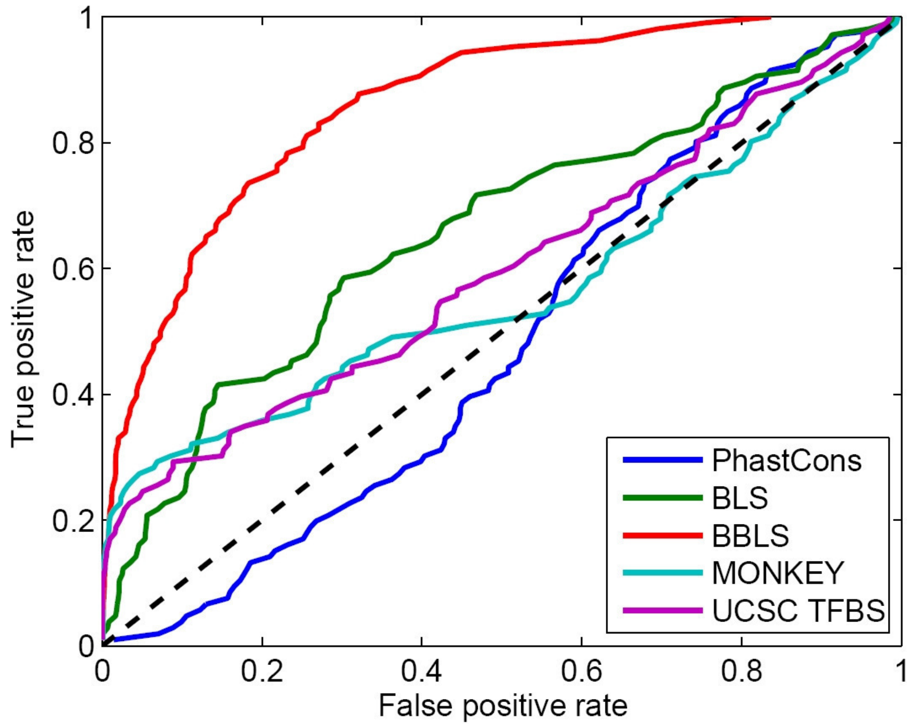

Figure S5 ROC curves of different methods for predicting **P53** binding sites. PhastCons: PhastCons conservation score; BLS: Branch length score; BBLS: Bayesian branch length score; MONKEY: Conservation p-value calculated by MONKEY (Moses et al., 2004); UCSC TFBS: Predicted sites from UCSC genome browser. Experimentally predicted P53 sites are from Wei et al. (2006).

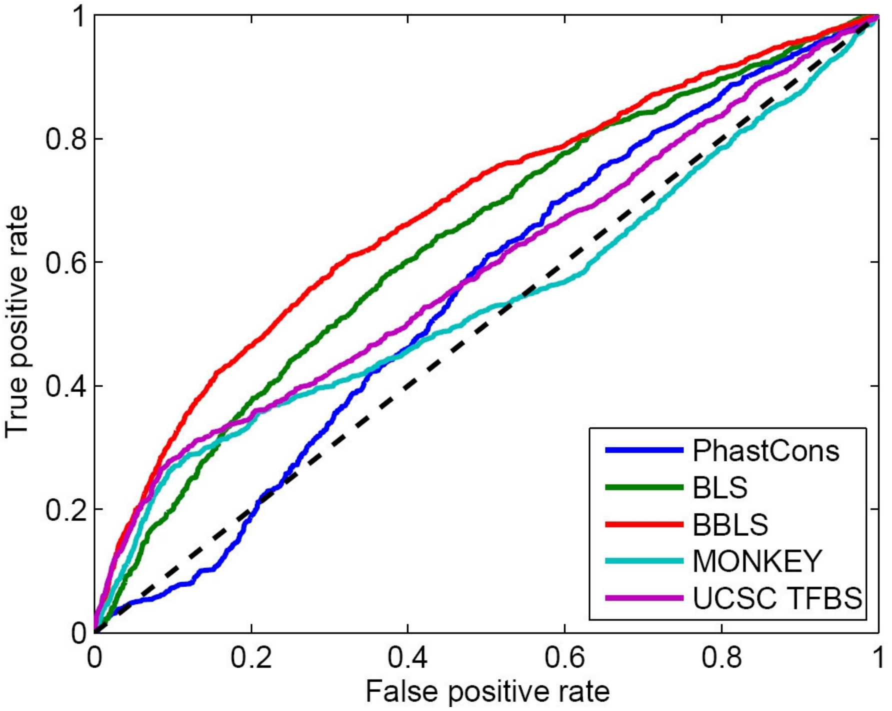

Figure S6 ROC curves of different methods for predicting **MYC** binding sites. PhastCons: PhastCons conservation score; BLS: Branch length score; BBLS: Bayesian branch length score; MONKEY: Conservation p-value calculated by MONKEY (Moses et al., 2004); UCSC TFBS: Predicted sites from UCSC genome browser. Experimentally identified MYC sites are from Zeller et al. (2006).

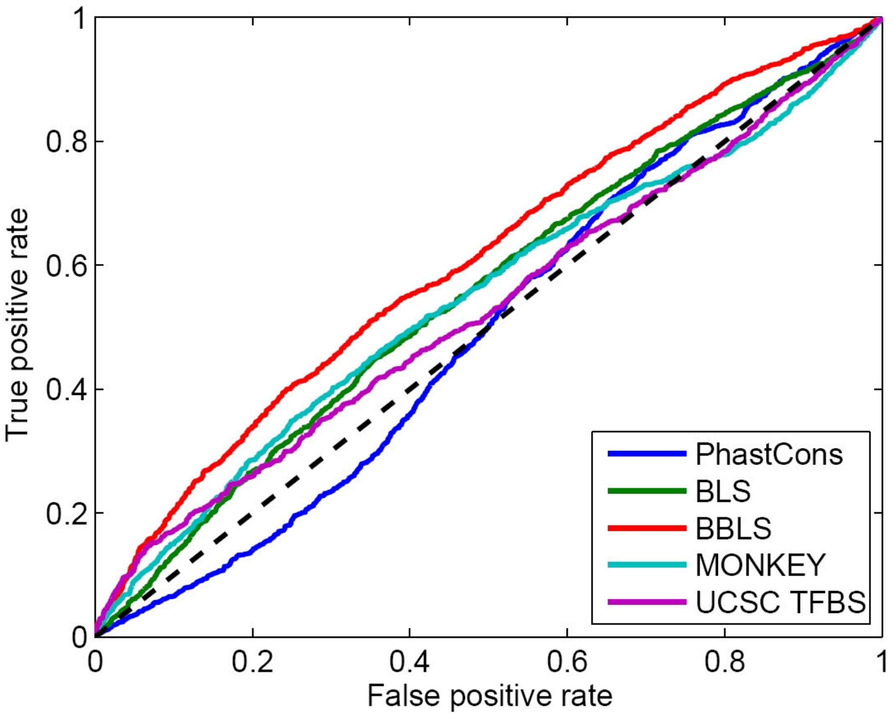

Figure S7 ROC curves of different methods for predicting **STAT1** binding sites. PhastCons: PhastCons conservation score; BLS: Branch length score; BBLS: Bayesian branch length score; MONKEY: Conservation p-value calculated by MONKEY (Moses et al., 2004); UCSC TFBS: Predicted sites from UCSC genome browser. Experimentally identified STAT1 sites are from Robertson et al. (2007).

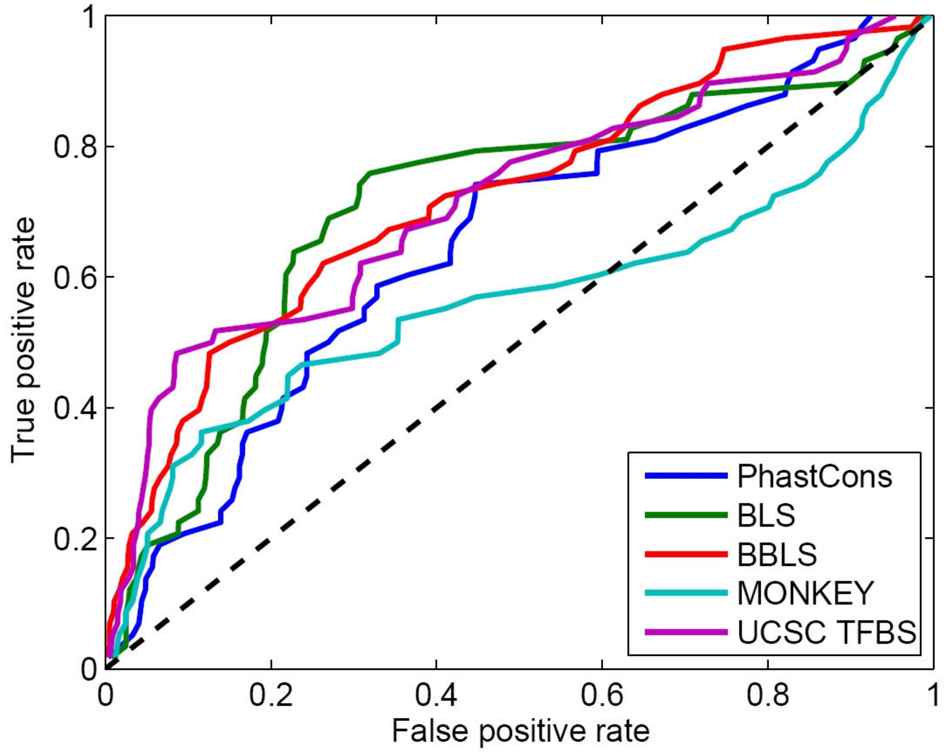

Figure S8 ROC curves of different methods for predicting **NF-kappaB** binding sites. PhastCons: PhastCons conservation score; BLS: Branch length score; BBLS: Bayesian branch length score; MONKEY: Conservation p-value calculated by MONKEY (Moses et al., 2004); UCSC TFBS: Predicted sites from UCSC genome browser. Experimentally identified NF-kappaB sites are from Lim et al. (2005).

Figure S9 MotifMap web server user interface

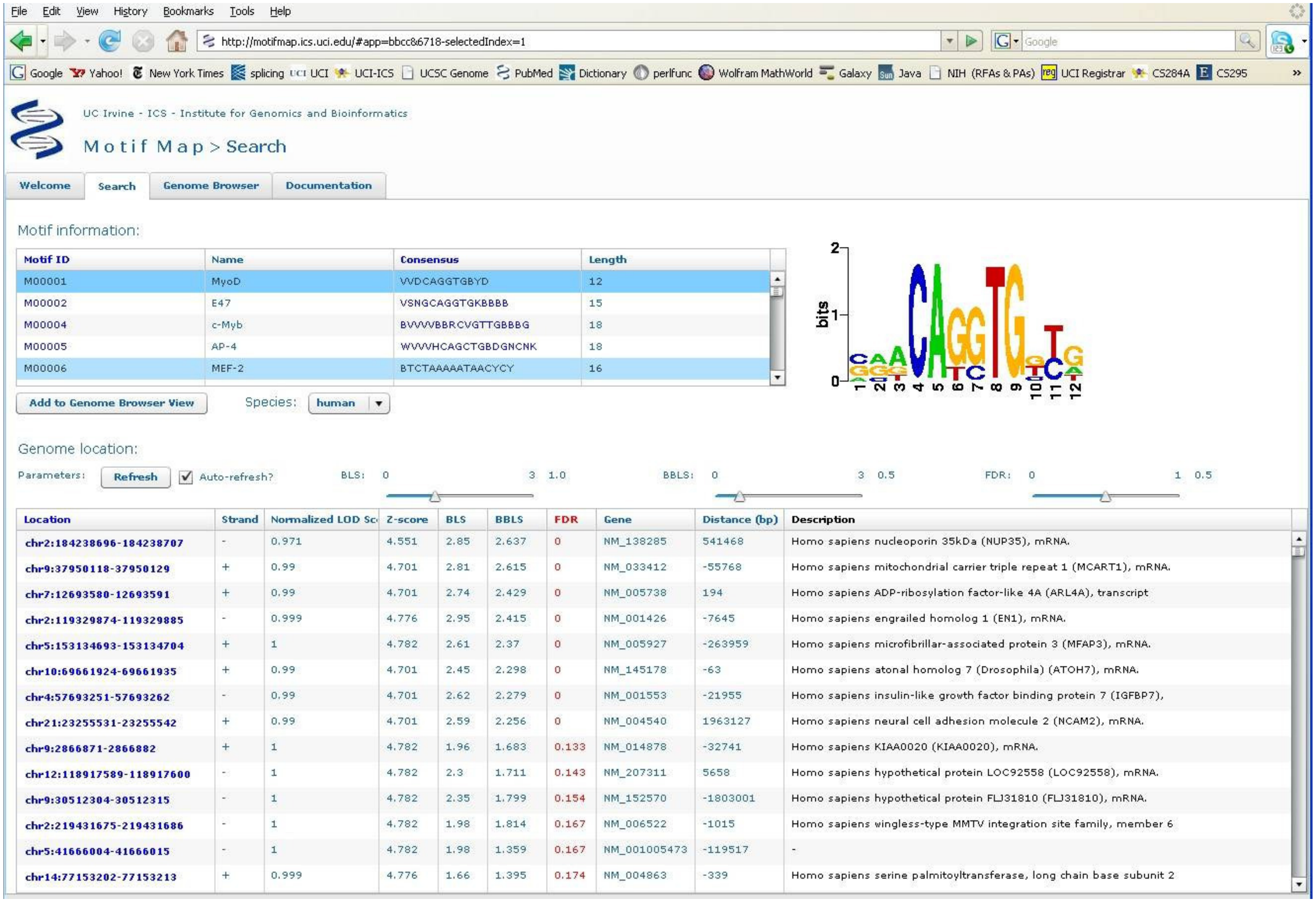

Motif information:

Motif ID	Name	Consensus	Length
M00001	MyoD	VVDCAGGTGBYD	12
M00002	E47	VSNGCAGGTGKBBBB	15
M00004	c-Myb	BVVVVBBRCVGTTGBBBG	18
M00005	AP-4	WVVVHCAGCTGBDGNCNK	18
M00006	MEF-2	BTCTAAAAATAACYCY	16

Add to Genome Browser View

Species: human

Genome location:

Parameters: Refresh ☑ Auto-refresh?

BLS: 0 3 1.0

BBLS: 0 3 0.5

FDR: 0 1 0.5

Location	Strand	Normalized LOD Sc	Z-score	BLS	BBLS	FDR	Gene	Distance (bp)	Description
chr2:184238696-184238707	-	0.971	4.551	2.85	2.637	0	NM_138285	541468	Homo sapiens nucleoporin 35kDa (NUP35), mRNA.
chr9:37950118-37950129	+	0.99	4.701	2.81	2.615	0	NM_033412	-55768	Homo sapiens mitochondrial carrier triple repeat 1 (MCART1), mRNA.
chr7:12693580-12693591	+	0.99	4.701	2.74	2.429	0	NM_005738	194	Homo sapiens ADP-ribosylation factor-like 4A (ARL4A), transcript
chr2:119329874-119329885	-	0.999	4.776	2.95	2.415	0	NM_001426	-7645	Homo sapiens engrailed homolog 1 (EN1), mRNA.
chr5:153134693-153134704	+	1	4.782	2.61	2.37	0	NM_005927	-263959	Homo sapiens microfibrillar-associated protein 3 (MFAP3), mRNA.
chr10:69661924-69661935	+	0.99	4.701	2.45	2.298	0	NM_145178	-63	Homo sapiens atonal homolog 7 (Drosophila) (ATOH7), mRNA.
chr4:57693251-57693262	-	0.99	4.701	2.62	2.279	0	NM_001553	-21955	Homo sapiens insulin-like growth factor binding protein 7 (IGFBP7),
chr21:23255531-23255542	+	0.99	4.701	2.59	2.256	0	NM_004540	1963127	Homo sapiens neural cell adhesion molecule 2 (NCAM2), mRNA.
chr9:2866871-2866882	+	1	4.782	1.96	1.683	0.133	NM_014878	-32741	Homo sapiens KIAA0020 (KIAA0020), mRNA.
chr12:118917589-118917600	-	1	4.782	2.3	1.711	0.143	NM_207311	5658	Homo sapiens hypothetical protein LOC92558 (LOC92558), mRNA.
chr9:30512304-30512315	-	1	4.782	2.35	1.799	0.154	NM_152570	-1803001	Homo sapiens hypothetical protein FLJ31810 (FLJ31810), mRNA.
chr2:219431675-219431686	-	1	4.782	1.98	1.814	0.167	NM_006522	-1015	Homo sapiens wingless-type MMTV integration site family, member 6
chr5:41666004-41666015	-	1	4.782	1.98	1.359	0.167	NM_001005473	-119517	-
chr14:77153202-77153213	+	0.999	4.776	1.66	1.395	0.174	NM_004863	-339	Homo sapiens serine palmitoyltransferase, long chain base subunit 2

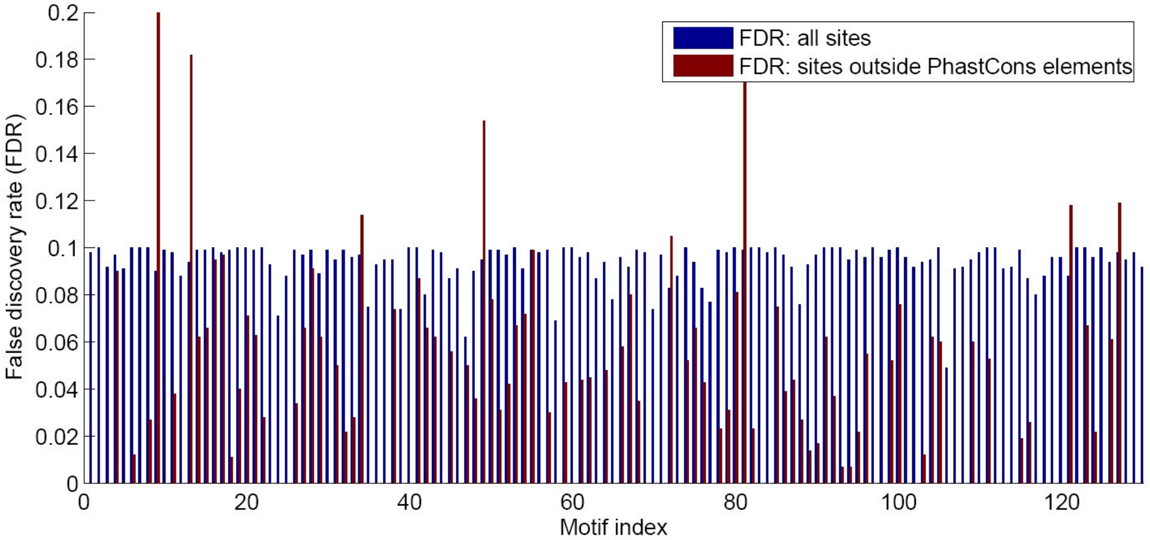

Figure S10 False discovery rates (FDR) of predicted motif sites. Each bar presents one motif. Blue: FDR based on all predicted sites; Red: FDR based only on sites outside PhastCons elements.

Supplementary Table S1 List of motifs with FDR ≤ 0.1

ID	Name	Number of sites	FDR	Motif score	BBLS
M00727	SF-1	15861	0.100	0.982	0.933
LM1_RFX1	LM1_RFX1	15319	0.098	0.767	0.500
LM2_CTCF	LM2_CTCF	12195	0.091	0.741	0.667
M00931	Sp1	10507	0.087	0.912	0.500
M00281	RFX1	8893	0.096	0.776	0.733
MA0004	Arnt	7434	0.098	0.874	1.433
M00925	AP-1	6513	0.100	0.906	1.167
M00510	Lhx3	5438	0.099	0.894	0.933
MA0093	USF1	5081	0.100	0.950	1.133
M00342	1-Oct	4769	0.099	0.943	1.500
M00173	AP-1	4607	0.099	0.957	0.500
M00652	Nrf-1	4035	0.100	0.900	0.600
MA0055	Myf	3808	0.098	0.858	0.967
M00025	Elk-1	3130	0.099	0.811	0.667
M00513	ATF3	3106	0.083	0.806	0.500
MA0076	ELK4	2777	0.099	0.903	0.867
M00532	RP58	2773	0.100	0.907	1.267
M00933	Sp1	2691	0.096	0.934	1.200
M01023	HSF1	2684	0.095	0.892	0.500
MA0058	MAX	2623	0.099	0.924	1.033
M00917	CREB	2482	0.099	0.825	0.833
M00039	CREB	2467	0.097	0.945	1.033
M00698	HEB	2415	0.100	0.989	1.867
M00041	CRE-BP1:c-Jun	2396	0.100	0.939	0.667
M00179	CRE-BP1	2381	0.100	0.893	0.567
LM4_M2	LM4_M2	2176	0.094	0.790	0.500
M00932	Sp1	2161	0.076	0.959	0.500
M00615	c-Myc:Max	2082	0.100	0.838	0.833
M00795	Octamer	2040	0.098	0.959	1.433
M00981	CREBATF	1931	0.099	0.959	0.933
M00287	NF-Y	1913	0.094	0.804	1.167
M00985	Stra13	1773	0.100	0.868	0.767
MA0060	NF-Y	1764	0.093	0.807	1.200
M01068	UF1H3BETA	1750	0.095	0.894	0.567
M00539	Arnt	1734	0.095	0.757	0.800
M00280	RFX1	1730	0.099	0.879	1.067
M00119	Max	1614	0.100	0.877	0.933
M00338	ATF	1610	0.097	0.900	0.800
M00465	POU6F1	1547	0.097	0.870	1.000
M00176	AP-4	1537	0.100	0.968	1.800
MA0062	GABPA	1426	0.097	0.936	0.933
LM9_NRSE	LM9_NRSE	1360	0.087	0.797	0.500
M00256	NRSF	1283	0.094	0.775	0.533
M00511	ERR	1276	0.080	0.976	0.500
M00070	Tal-1beta:ITF-2	1215	0.100	0.890	1.133
M00418	TGIF	1160	0.100	0.956	1.700
MA0088	Staf	1146	0.099	0.893	0.533
M01028	NRSF	1110	0.099	0.827	0.600
M00916	CREB	1086	0.099	0.800	1.067
M00121	USF	1034	0.099	0.912	0.933
M00032	c-Ets-1(p54)	941	0.091	0.970	1.467
M00177	CREB	894	0.096	0.814	1.200
M00279	MIF-1	880	0.100	0.850	1.000
M00325	neural-restr.-silencer-element	863	0.095	0.808	0.500
M01035	YY1	859	0.100	0.950	1.133
M00231	MEF-2	744	0.099	0.767	1.067
M00178	CREB	741	0.100	0.958	0.933
M00037	NF-E2	700	0.097	0.988	0.833
M00017	ATF	665	0.096	0.903	1.000
MA0091	TAL1-TCF3	651	0.095	0.944	1.567
M01058	GFI1B	622	0.100	0.945	0.933
M00187	USF	546	0.099	0.995	0.500
M00639	HNF-6	535	0.097	0.992	0.867
MA0065	PPARG-RXRA	523	0.096	0.830	0.933
M00420	MEIS1A:HOXA9	505	0.095	0.895	1.133
M00210	OCT-x	502	0.100	0.902	1.667
M00821	Nrf2	457	0.096	0.934	1.367
M01031	HNF4	446	0.094	0.827	1.500
M00174	AP-1	443	0.099	0.994	1.200
M00941	MEF-2	442	0.100	0.895	1.467
M00118	c-Myc:Max	420	0.100	0.897	0.533
M00188	AP-1	420	0.095	0.964	1.700
M00793	YY1	411	0.092	0.986	1.867
M00775	NF-Y	406	0.099	0.982	0.767
M00339	c-Ets-1	404	0.089	0.965	0.500
M00641	HSF	399	0.100	0.978	0.500
MA0028	ELK1	394	0.096	0.879	1.833
MA0017	NR2F1	387	0.098	0.914	1.333
M00196	Sp1	381	0.100	0.957	1.367
M00691	ATF-1	379	0.100	0.967	0.667

M00526	GCNF	371	0.097	0.891	0.500
M00762	PPAR,	368	0.098	0.912	1.467
M00341	GABP	368	0.092	0.942	1.300
M00771	ETS	367	0.098	0.975	1.167
M00437	CHX10	324	0.099	0.796	1.633
M00161	1-Oct	306	0.098	0.940	1.667
M00774	NF-kappaB	304	0.092	0.899	1.333
M00065	Tal-1beta:E47	285	0.098	0.880	1.467
MA0059	MYC-MAX	284	0.092	0.955	0.867
M00517	AP-1	279	0.100	0.954	1.500
M00930	1-Oct	261	0.100	0.891	2.167
MA0114	HNF4	258	0.093	0.939	1.533
M00514	ATF4	253	0.095	0.950	1.100
M00512	PPARG	245	0.090	0.848	0.900
M00224	STAT1	240	0.100	0.850	0.500
M00138	1-Oct	239	0.075	0.828	0.867
M00122	USF	228	0.088	0.968	1.200
M00528	PPAR	223	0.090	0.753	1.333
M00421	MEIS1B:HOXA9	220	0.100	0.939	1.467
M00799	Myc	212	0.094	0.883	2.600
M00763	PPAR	202	0.099	0.969	1.000
M00069	YY1	197	0.091	0.850	1.067
M00113	CREB	195	0.092	0.808	1.567
M00626	RFX1	188	0.096	0.947	1.033
M00157	RORalpha2	181	0.088	0.827	2.133
M00993	TAL1	171	0.094	0.994	2.233
M00066	Tal-1alpha:E47	160	0.100	0.906	1.667
M00193	NF-1	160	0.100	0.934	1.300
M00184	MyoD	160	0.100	0.889	2.467
M00236	Arnt	151	0.093	0.785	1.400
M00927	AP-4	145	0.097	0.996	2.433
M00175	AP-4	144	0.097	0.999	1.800
M00796	USF	144	0.097	0.961	1.233
M00972	IRF	143	0.098	0.907	1.667
M00108	NRF-2	137	0.088	0.976	1.667
M00965	LXR,	133	0.090	0.910	0.900
M00765	COUP	131	0.092	0.916	1.667
M00135	1-Oct	128	0.094	0.901	1.700
M01036	COUPTF	125	0.096	0.846	1.000
M00516	E2F	123	0.098	0.957	0.833
M00982	KROX	122	0.049	0.977	0.500
MA0107	RELA	107	0.093	0.996	2.233
M00405	MEF-2	102	0.098	0.940	0.967
M00220	SREBP-1	102	0.098	0.965	1.400
M00407	RSRFC4	101	0.099	0.952	1.000
M00134	HNF-4	101	0.099	0.899	1.300
M01022	LEF1	100	0.100	0.986	2.167
M00983	MAF	100	0.100	0.985	2.000
M00006	MEF-2	96	0.083	0.920	1.033
MA0115	NR1H2-RXR	91	0.088	0.875	1.033
M00422	FOXJ2	89	0.090	0.903	1.633
M00638	HNF-4alpha	89	0.090	0.950	1.867
M00084	MZF1	87	0.069	0.992	0.767
M01012	HNF3	84	0.071	0.941	1.133
M00450	Zic3	84	0.095	0.862	2.567
M00978	LEF1TCF1	83	0.096	0.990	2.300
M00649	MAZ	82	0.098	0.960	2.633
MA0113	NR3C1	81	0.099	0.939	0.733
M00406	MEF-2	78	0.077	0.945	1.067
M00922	SRF	69	0.087	0.931	1.533
MA0007	Ar	68	0.088	0.897	0.800
M00457	STAT5A	68	0.088	0.978	1.000
M00920	E2F	66	0.091	0.952	1.033
M00007	Elk-1	66	0.091	0.954	0.867
M00225	STAT3	65	0.092	0.882	0.600
M00460	STAT5A	65	0.062	0.887	0.500
M00284	TCF11:MafG	64	0.094	0.862	1.333
M00005	AP-4	64	0.094	0.951	0.500
M00764	HNF-4	63	0.095	0.984	0.967
MA0119	Hox11-CTF1	62	0.097	0.898	1.767
MA0072	RORA1	60	0.100	0.984	1.933
M00518	PPARalpha:RXR-alpha	54	0.074	0.910	1.167
M00411	HNF-4alpha1	54	0.074	0.962	1.100
M00448	Zic1	53	0.075	0.883	2.567
MA0018	CREB1	51	0.078	0.966	1.633
M00956	AR	50	0.080	0.850	0.833
M00378	Pax-4	50	0.080	0.896	1.967

Supplementary Table S2 List of motifs with FDR ≤ 0.5

ID	Name	Number of sites	FDR	Motif score	BBLS
M00993	TAL1	37249	0.449	0.864	0.500
M00727	SF-1	25115	0.289	0.872	0.500
M00698	HEB	22752	0.305	0.849	0.500
M00342	1-Oct	20695	0.267	0.853	0.500
M00199	AP-1	17887	0.494	0.900	0.500
JASPAR_MA0071	RORA	16777	0.427	0.853	0.500
M00933	Sp1	16575	0.439	0.804	0.500
M00749	SREBP-1	16561	0.484	0.877	0.500
M00511	ERR	16410	0.382	0.836	0.500
LM1_RFX1	LM1_RFX1	15579	0.102	0.707	0.500
TBX	TBX	15392	0.324	0.877	0.500
LM2_CTCF	LM2_CTCF	15245	0.163	0.741	0.500
M00649	MAZ	14385	0.398	0.860	0.500
M00176	AP-4	13578	0.299	0.878	0.500
M00973	E2A	13549	0.462	0.978	0.500
M00196	Sp1	13484	0.398	0.777	0.500
M00418	TGIF	13410	0.249	0.856	0.500
M00532	RP58	13217	0.268	0.817	0.500
JASPAR_MA0002	RUNX1	13064	0.500	0.894	1.000
M00931	Sp1	13035	0.327	0.782	0.500
M00932	Sp1	12886	0.392	0.779	0.500
JASPAR_MA0093	USF1	12857	0.135	0.840	0.500
M00722	core-binding	12817	0.494	0.908	1.133
M00281	RFX1	12639	0.174	0.776	0.500
JASPAR_MA0104	Mycn	12638	0.302	0.867	0.500
JASPAR_MA0004	Arnt	12463	0.130	0.874	0.500
M00174	AP-1	12055	0.500	0.864	0.600
M00490	Bach2	11970	0.498	0.822	0.533
JASPAR_MA0091	TAL1-TCF3	11930	0.276	0.834	0.500
M00437	CHX10	11399	0.408	0.796	0.500
M00517	AP-1	11334	0.305	0.824	0.500
M00037	NF-E2	11290	0.311	0.828	0.500
M00070	Tal-1beta:ITF-2	11239	0.280	0.780	0.500
JASPAR_MA0031	FOXD1	11171	0.498	0.906	1.167
M00925	AP-1	10942	0.157	0.906	0.500
M00457	STAT5A	10824	0.265	0.828	0.500
M00065	Tal-1beta:E47	10599	0.283	0.770	0.500
M00720	CAC-binding	10393	0.143	0.901	0.500
M00795	Octamer	10167	0.202	0.879	0.500
M00066	Tal-1alpha:E47	10105	0.300	0.796	0.500
JASPAR_MA0006	Arnt-Ahr	9589	0.482	0.878	0.500
M00695	ETF	9574	0.441	0.992	0.500
M00495	Bach1	9534	0.486	0.766	0.500
M00210	OCT-x	9470	0.378	0.812	0.500
M00775	NF-Y	9266	0.275	0.852	0.500
JASPAR_MA0119	Hox11-CTF1	8908	0.375	0.728	0.500
M00652	Nrf-1	8906	0.334	0.750	0.500
JASPAR_MA0099	Fos	8905	0.483	0.911	0.500
M00806	NF-1	8780	0.477	0.802	0.500
JASPAR_MA0055	Myf	8623	0.196	0.858	0.500
M01058	GFI1B	8566	0.216	0.815	0.500
M00793	YY1	8542	0.377	0.886	0.500
M00459	STAT5B	8492	0.288	0.816	0.500
M00188	AP-1	8379	0.499	0.864	0.567
M00008	Sp1	8338	0.497	0.861	0.600
M00157	RORalpha2	8328	0.494	0.897	0.600
M00055	N-Myc	8210	0.457	0.790	0.500
M00510	Lhx3	8119	0.128	0.894	0.500
JASPAR_MA0072	RORA1	8018	0.476	0.824	0.633
M00135	1-Oct	7775	0.303	0.781	0.500
M00193	NF-1	7684	0.406	0.794	0.500
M00771	ETS	7681	0.231	0.855	0.500
JASPAR_MA0114	HNF4	7650	0.305	0.829	0.500
JASPAR_MA0090	TEAD	7550	0.219	0.822	0.500
M00287	NF-Y	7541	0.340	0.804	0.500
M00032	c-Ets-1(p54)	7538	0.321	0.880	0.500
JASPAR_MA0060	NF-Y	7516	0.493	0.807	0.500
M01031	HNF4	7503	0.252	0.827	0.500
M00052	NF-kappaB	7429	0.499	0.836	0.833
M00002	E47	7296	0.456	0.817	0.500
M00651	NF-muE1	7190	0.495	0.886	0.667
JASPAR_MA0048	NHLH1	7033	0.454	0.779	0.500
M00804	E2A	7023	0.428	0.830	0.500
M00223	STATx	6964	0.132	0.876	0.500
JASPAR_MA0107	RELA	6752	0.495	0.916	0.767
JASPAR_MA0058	MAX	6728	0.178	0.824	0.500
M00280	RFX1	6604	0.394	0.789	0.500
M00924	AP-1	6596	0.499	0.853	0.567
M00799	Myc	6524	0.215	0.883	0.500
M00421	MEIS1B:HOXA9	6460	0.469	0.799	0.600

M00277	Lmo2	6456	0.385	0.858	0.500
M00774	NF-kappaB	6439	0.381	0.789	0.500
M00121	USF	6438	0.349	0.772	0.500
M00762	PPAR,	6389	0.354	0.822	0.500
JASPAR_MA0059	MYC-MAX	6366	0.391	0.785	0.500
M00175	AP-4	6253	0.263	0.899	0.500
M01034	Ebox	6225	0.500	0.941	0.633
M00340	c-Ets-2	6118	0.386	0.864	0.500
M00927	AP-4	6036	0.227	0.906	0.500
M00217	USF	5999	0.353	0.872	0.500
M00641	HSF	5983	0.273	0.788	0.500
M00639	HNF-6	5981	0.401	0.892	0.500
M00187	USF	5975	0.390	0.855	0.500
M00481	AR	5975	0.500	0.756	0.533
M00701	SMAD-3	5926	0.497	0.978	0.767
M00978	LEF1TCF1	5921	0.491	0.890	0.733
M00778	AhR	5917	0.468	0.809	0.500
M00136	1-Oct	5894	0.469	0.836	0.500
M00930	1-Oct	5809	0.209	0.891	0.500
M00341	GABP	5785	0.352	0.812	0.500
M00339	c-Ets-1	5779	0.228	0.845	0.500
M00414	AREB6	5627	0.491	0.828	0.767
M00982	KROX	5609	0.491	0.817	0.500
NKX25_V2	NKX25_	5590	0.496	0.826	0.567
M00420	MEIS1A:HOXA9	5583	0.286	0.785	0.500
M00173	AP-1	5497	0.120	0.877	0.500
M00615	c-Myc:Max	5442	0.203	0.748	0.500
M01068	UF1H3BETA	5418	0.367	0.724	0.500
M00531	NERF1a	5318	0.243	0.805	0.500
M00231	MEF-2	5254	0.246	0.767	0.500
M00981	CREBATF	5249	0.216	0.839	0.500
M00026	RSRFC4	5240	0.480	0.813	0.500
M00528	PPAR	5170	0.378	0.753	0.500
M00108	NRF-2	5151	0.388	0.836	0.500
JASPAR_MA0062	GABPA	5151	0.268	0.836	0.500
M00821	Nrf2	5081	0.302	0.834	0.500
M00246	Egr-2	4972	0.406	0.745	0.500
M00184	MyoD	4965	0.479	0.889	1.067
M00119	Max	4796	0.163	0.787	0.500
M00769	AML	4749	0.491	0.829	0.700
M00619	Alx-4	4723	0.396	0.709	0.500
M00691	ATF-1	4713	0.448	0.817	0.500
M00985	Stra13	4596	0.212	0.778	0.500
M01022	LEF1	4593	0.438	0.896	0.500
M00763	PPAR	4582	0.463	0.839	0.500
M01035	YY1	4566	0.426	0.850	0.500
JASPAR_MA0065	PPARG-RXRA	4541	0.357	0.710	0.500
M00526	GCNF	4424	0.262	0.721	0.500
M00161	1-Oct	4407	0.285	0.860	0.500
JASPAR_MA0115	NR1H2-RXR	4285	0.477	0.695	0.500
M00765	COUP	4284	0.482	0.786	0.700
M00338	ATF	4282	0.279	0.780	0.500
M00678	Tel-2	4279	0.495	0.923	0.800
JASPAR_MA0076	ELK4	4278	0.184	0.813	0.500
M00258	ISRE	4232	0.413	0.779	0.500
M00005	AP-4	4164	0.310	0.791	0.500
M00449	Zic2	4159	0.495	0.914	0.667
M01023	HSF1	4101	0.130	0.812	0.500
M00006	MEF-2	4060	0.390	0.760	0.500
M00025	Elk-1	4037	0.125	0.811	0.500
M00406	MEF-2	4023	0.349	0.785	0.500
M00232	MEF-2	4009	0.481	0.778	0.567
M00512	PPARG	3987	0.308	0.698	0.500
M00071	E47	3959	0.485	0.814	0.767
M01047	AP-2alphaA	3954	0.475	0.752	0.500
M00194	NF-kappaB	3877	0.489	0.805	0.633
M00039	CREB	3839	0.195	0.845	0.500
M00178	CREB	3825	0.300	0.818	0.500
M00118	c-Myc:Max	3772	0.314	0.747	0.500
M00017	ATF	3770	0.306	0.783	0.500
M00539	Arnt	3676	0.176	0.757	0.500
M00917	CREB	3657	0.182	0.825	0.500
M00983	MAF	3655	0.401	0.875	0.500
M00411	HNF-4alpha1	3633	0.486	0.772	0.700
M00959	ER	3629	0.497	0.842	0.767
JASPAR_MA0050	IRF1	3628	0.398	0.839	0.500
M00929	MyoD	3581	0.342	0.775	0.500
M00378	Pax-4	3559	0.229	0.896	0.500
M00693	E12	3552	0.498	0.931	0.933
JASPAR_MA0017	NR2F1	3546	0.215	0.844	0.500
M00158	COUP-TF,	3546	0.455	0.844	0.500
M00195	1-Oct	3543	0.470	0.842	0.733
M00483	ATF6	3498	0.463	0.795	0.500
M00243	Egr-1	3492	0.497	0.752	0.533

M00123	c-Myc:Max	3454	0.490	0.904	0.700
M00279	MIF-1	3431	0.413	0.750	0.500
M00407	RSRFC4	3425	0.307	0.822	0.500
M00916	CREB	3424	0.192	0.800	0.500
LM4_M2	LM4_M2	3343	0.252	0.670	0.500
M00244	NGFI-C	3334	0.499	0.837	0.500
M00465	POU6F1	3299	0.178	0.870	0.500
M00113	CREB	3296	0.359	0.808	0.500
M00236	Arnt	3291	0.292	0.785	0.500
M00746	ELF-1	3207	0.279	0.890	0.500
M00209	NF-Y	3203	0.485	0.800	0.800
M00513	ATF3	3106	0.083	0.806	0.500
M00284	TCF11:MafG	3094	0.434	0.752	0.500
M00134	HNF-4	3059	0.237	0.799	0.500
M00476	FOXO4	2994	0.497	0.822	0.633
M00177	CREB	2979	0.242	0.814	0.500
M01019	TBX5	2964	0.496	0.883	1.167
M00084	MZF1	2913	0.500	0.922	0.567
M00001	MyoD	2802	0.491	0.869	0.800
M00041	CRE-BP1:c-Jun	2792	0.145	0.839	0.500
M00424	NKX6-1	2780	0.333	0.860	0.500
M00772	IRF	2738	0.362	0.868	0.500
M00099	S8	2736	0.491	0.845	0.667
M00179	CRE-BP1	2700	0.123	0.823	0.500
JASPAR_MA0052	MEF2A	2673	0.497	0.855	1.167
M00220	SREBP-1	2668	0.500	0.795	0.867
M00122	USF	2660	0.217	0.868	0.500
M00416	Cart-1	2644	0.478	0.806	0.500
M00777	STAT	2635	0.216	0.877	0.500
JASPAR_MA0018	CREB1	2630	0.365	0.826	0.500
JASPAR_MA0051	IRF2	2598	0.467	0.774	0.500
M00069	YY1	2588	0.242	0.750	0.500
M00225	STAT3	2515	0.256	0.722	0.500
M00433	Hmx3	2477	0.379	0.868	0.500
M00333	ZF5	2452	0.303	0.812	0.500
M00185	NF-Y	2380	0.497	0.881	1.200
M01028	NRSF	2368	0.258	0.717	0.500
M00172	AP-1	2342	0.491	0.951	0.900
JASPAR_MA0028	ELK1	2338	0.312	0.879	0.500
M00292	Freac-4	2303	0.489	0.814	0.600
M00208	NF-kappaB	2238	0.495	0.867	0.867
JASPAR_MA0088	Staf	2234	0.167	0.813	0.500
M00796	USF	2230	0.436	0.851	0.500
M00007	Elk-1	2225	0.332	0.834	0.500
M01013	IPF1	2215	0.427	0.839	0.500
LM9_NRSE	LM9_NRSE	2159	0.380	0.657	0.500
M00224	STAT1	2157	0.172	0.720	0.500
M00460	STAT5A	2153	0.256	0.727	0.500
M00054	NF-kappaB	2148	0.490	0.833	1.333
JASPAR_MA0038	Gfi	2143	0.153	0.916	0.500
M00699	ICSBP	2142	0.499	0.847	0.833
M00250	Gfi-1	2124	0.332	0.784	0.500
M00764	HNF-4	2110	0.493	0.894	0.933
M00261	Olf-1	2053	0.375	0.802	0.500
M00638	HNF-4alpha	2053	0.496	0.860	0.700
M00965	LXR,	2039	0.495	0.790	0.533
M00706	TFII-I	2033	0.488	0.994	1.233
M00290	Freac-2	2028	0.477	0.811	0.800
M00245	Egr-3	1958	0.499	0.846	0.600
M00790	HNF-1	1925	0.361	0.797	0.500
M00256	NRSF	1910	0.287	0.655	0.500
M00955	GR	1889	0.425	0.728	0.500
M00068	HEN1	1879	0.456	0.787	0.500
M01037	GLI	1798	0.493	0.816	1.067
JASPAR_MA0070	Pbx	1790	0.494	0.823	1.167
M00953	AR	1789	0.345	0.707	0.500
M01066	BLIMP1	1788	0.493	0.847	0.567
M00464	POU3F2	1784	0.494	0.850	1.367
M00325	neural-restr.-silencer-element	1779	0.302	0.688	0.500
JASPAR_MA0105	NFKB1	1765	0.479	0.798	1.000
M00740	Rb:E2F-1:DP-1	1759	0.314	0.844	0.500
M00419	MEIS1	1722	0.496	0.844	1.133
M00156	RORalpha1	1699	0.491	0.937	1.067
M00956	AR	1696	0.439	0.710	0.500
M00302	NF-AT	1692	0.307	0.916	0.500
M00450	Zic3	1692	0.480	0.862	1.367
M00941	MEF-2	1679	0.211	0.895	0.500
M00725	HP1	1648	0.424	0.874	0.500
M00448	Zic1	1641	0.491	0.973	0.900
M00984	PEBP	1620	0.498	0.809	0.967
JASPAR_MA0101	REL	1619	0.499	0.842	1.400
JASPAR_MA0079	SP1	1607	0.494	0.952	0.767
M00687	alpha-CP1	1600	0.500	0.853	1.033

M00922	SRF	1561	0.495	0.801	0.800
M00053	c-Rel	1527	0.492	0.951	1.267
M00742	HFH-4	1501	0.485	0.836	0.967
M00808	Pax	1493	0.496	0.944	0.500
M00132	HNF-1	1472	0.496	0.822	0.700
M00087	Ik-2	1429	0.470	0.974	0.500
JASPAR_MA0007	Ar	1333	0.495	0.827	0.533
M01036	COUPTF	1274	0.265	0.786	0.500
M00058	HEN1	1258	0.491	0.785	0.500
M00124	Pbx1b	1250	0.477	0.786	1.100
JASPAR_MA0024	E2F1	1235	0.483	0.842	0.500
M00248	1-Oct	1232	0.490	0.847	1.367
M01067	GFI1	1231	0.310	0.860	0.500
M00436	IPF1	1203	0.499	0.873	1.000
M00976	AHRHIF	1182	0.496	0.973	0.500
M00998	PBX	1172	0.491	0.876	1.033
M00737	E2F-1:DP-2	1167	0.494	0.869	0.567
M00694	E4F1	1155	0.495	0.822	0.533
M00251	XBP-1	1135	0.446	0.768	0.500
M00514	ATF4	1131	0.308	0.870	0.500
M00034	p53	1097	0.463	0.651	0.500
M00453	IRF-7	1062	0.243	0.808	0.500
M00738	E2F-4:DP-1	1027	0.495	0.830	0.767
M00233	MEF-2	1013	0.494	0.804	0.533
M00097	Pax-6	1008	0.345	0.763	0.500
M00051	NF-kappaB	1000	0.500	0.788	1.200
M00920	E2F	977	0.497	0.832	0.500
M00516	E2F	945	0.408	0.827	0.500
M00939	E2F-1	888	0.419	0.853	0.500
M00403	aMEF-2	868	0.309	0.841	0.500
M00033	p300	858	0.492	0.927	0.500
M00918	E2F	841	0.407	0.861	0.500
M00186	SRF	826	0.494	0.886	1.033
M00626	RFX1	796	0.291	0.867	0.500
M00648	MAF	793	0.494	0.812	0.700
M00919	E2F	786	0.458	0.845	0.500
M00915	AP-2	756	0.484	0.970	0.500
M00736	E2F-1:DP-1	740	0.351	0.894	0.500
M00972	IRF	738	0.268	0.907	0.500
M00206	HNF-1	722	0.493	0.910	0.567
M00138	1-Oct	711	0.138	0.828	0.500
M00422	FOXJ2	702	0.245	0.903	0.500
M00332	Whn	693	0.491	0.931	0.500
M00974	SMAD	685	0.491	0.966	1.167
JASPAR_MA0113	NR3C1	675	0.249	0.849	0.500
M00413	AREB6	674	0.496	0.943	1.233
M01045	AP-2alphaA	673	0.487	0.814	1.033
M00145	Brn-2	670	0.463	0.920	0.500
JASPAR_MA0106	TP53	660	0.442	0.686	0.567
M00024	E2F	630	0.422	0.766	0.500
M00474	FOXO1	625	0.499	0.893	1.233
JASPAR_MA0061	NF-kappaB	598	0.495	0.834	1.867
M00954	PR	563	0.497	0.708	0.633
M01011	HNF1	559	0.494	0.791	0.800
M00447	AR	548	0.496	0.915	0.800
M00739	E2F-4:DP-2	539	0.494	0.973	1.033
JASPAR_MA0083	SRF	528	0.496	0.829	1.167
M00940	E2F-1	528	0.455	0.865	0.500
M01017	PBX1	527	0.482	0.891	1.367
M00947	CP2/LBP-1c/LSF	523	0.455	0.931	0.500
M00106	CDP	520	0.496	0.888	0.733
M00056	myogenin	508	0.402	0.756	0.500
M01007	SRF	495	0.469	0.765	1.033
M01012	HNF3	490	0.384	0.871	0.500
M00291	Freac-3	483	0.497	0.890	1.267
M00289	HFH-3	481	0.486	0.891	0.933
M00430	E2F-1	473	0.499	0.985	1.400
M00485	Nkx2-2	469	0.499	0.982	1.600
M00634	GCM	446	0.484	0.906	1.067
M00128	GATA-1	445	0.494	0.891	0.867
M00405	MEF-2	444	0.239	0.870	0.500
M00425	E2F	439	0.497	0.832	1.167
M00104	CDP	427	0.482	0.911	1.000
M00426	E2F	410	0.395	0.899	0.500
M00518	PPARalpha:RXR-alpha	410	0.498	0.860	0.800
M00050	E2F	405	0.499	0.952	0.833
M00729	Cdx-2	394	0.487	0.893	0.733
M00484	Ncx	385	0.483	0.875	0.867
JASPAR_MA0068	Pax4	384	0.292	0.747	0.500
M00622	C/EBPgamma	381	0.189	0.920	0.500
JASPAR_MA0077	SOX9	364	0.456	0.875	2.133
M00192	GR	363	0.479	0.882	0.900
M00427	E2F	361	0.283	0.903	0.500

M00979	PAX6	350	0.497	0.901	0.567
M00045	E4BP4	341	0.499	0.936	1.433
M00063	IRF-2	340	0.482	0.782	1.267
JASPAR_MA0066	PPARG	338	0.491	0.830	0.533
M00242	PPARalpha:RXR-alpha	323	0.495	0.823	0.767
M00205	GR	312	0.494	0.908	0.900
M00215	SRF	300	0.493	0.789	1.267
M00957	PR	286	0.483	0.696	0.800
M00477	FOXO3	276	0.486	0.838	1.500
M00766	LXR	267	0.427	0.725	1.133
M00079	Evi-1	265	0.483	0.970	1.567
M01044	TBX5	264	0.492	0.804	1.900
M00131	HNF-3beta	256	0.492	0.896	1.200
M00733	SMAD-4	255	0.486	0.834	1.200
M00380	Pax-4	236	0.305	0.752	0.500
M00647	LXR	214	0.495	0.823	0.967
M00004	c-Myb	213	0.469	0.851	0.900
M00257	RREB-1	213	0.272	0.961	0.500
M00088	Ik-3	213	0.498	0.959	0.767
M00809	FOX	211	0.493	0.907	1.000
M00062	IRF-1	209	0.498	0.930	1.033
M01020	TBX5	204	0.490	0.922	1.100
M00480	LUN-1	196	0.500	0.821	0.633
M00059	YY1	185	0.497	0.867	0.967
M00472	FOXO4	184	0.489	0.918	1.100
M00346	GATA-1	182	0.495	0.894	2.100
M00538	HTF	182	0.484	0.836	0.733
JASPAR_MA0040	Foxq1	180	0.500	0.987	1.800
M00463	POU3F2	180	0.500	0.958	1.000
M00810	SRF	177	0.475	0.893	1.033
M00466	HIF-1	173	0.497	0.914	1.033
M00150	Brachyury	154	0.494	0.775	0.667
M00665	Sp3	151	0.384	0.965	0.500
M00410	SOX-9	148	0.473	0.954	1.600
M00794	TTF-1	147	0.490	0.887	1.300
M00717	Pax-8	146	0.479	0.885	0.900
M00075	GATA-1	129	0.434	0.906	0.500
M00130	FOXD3	126	0.492	0.926	0.600
JASPAR_MA0112	ESR1	120	0.483	0.831	1.167
M00987	FOXP1	119	0.471	0.902	0.500
M00137	1-Oct	118	0.458	0.884	0.700
M00797	HIF-1	117	0.462	0.858	1.267
JASPAR_MA0009	T	106	0.491	0.873	1.700
M00183	c-Myb	101	0.495	0.903	2.200
JASPAR_MA0073	RREB1	92	0.500	0.920	0.500
M00203	GATA-X	87	0.460	0.913	1.500
M00444	VDR	87	0.483	0.865	1.233
JASPAR_MA0042	FOXI1	85	0.447	0.993	1.033
M00456	FAC1	81	0.469	0.955	0.567
M00807	EGR	79	0.481	0.966	1.733
M00721	CACCC-binding	77	0.494	0.940	0.933
M00646	LF-A1	76	0.447	0.910	2.567
M00129	HFH-1	76	0.500	0.990	1.867
M00057	COMP1	70	0.486	0.839	0.633
M00235	AhR:Arnt	69	0.493	0.885	1.067
M00294	HFH-8	69	0.493	0.960	2.067
M00214	SEF-1	67	0.478	0.813	0.733
M00631	FXR/RXR-alpha	66	0.485	0.935	1.200
TBX_V2	TBX	60	0.433	0.702	1.000
M00191	ER	56	0.500	0.922	0.633
M01072	HIC1	55	0.473	0.957	0.500
M00515	PPARG	50	0.400	0.799	0.900